Atomic force microscopy characterization of printed dots

Maria J Cadena[1,2], Ronald Reifenberger[2,3], Jan P Allebach[4], Arvind Raman[1,2]
[1]School of Mechanical Engineering, [2]Birck Nanotechnology Center, [3]Department of Physics, [4]School of Electrical and Computer Engineering; Purdue University, West Lafayette, IN 47907, USA.

Abstract

Functional atomic force microscopy (AFM) techniques are proposed as a high resolution tool to understand relevant physical properties of colorants and printing substrates at nanoscale. In this work, we present an exploratory AFM study of colorants used by three digital printing technologies: LaserJet, Indigo, inkjet and two printing substrates: white paper and transparent media. Surface morphology and phase-contrast imaging are performed using amplitude-modulation (AM) AFM and measurements of surface potential and capacitance gradient are measured through 2nd harmonic Kelvin Probe Force microscopy (KPFM). Compositional mapping contrast is analyzed using both techniques. Non-homogeneous mechanical properties are clearly evident in the AM-AFM images while the variations of local electrical properties are apparent from the KPFM studies.

Introduction

The use of printers to rapidly produce documents is a practice common to all levels of society. Each machine/process that produces printed copy is different and has unique limitations. In order to achieve continuous quality improvement, new ways to characterize and better understand the physical properties of colorants printed onto different substrates are of general interest to the printing industry.

Colorants, such as toners or inks, are complex materials that in general are composed of pigments, binder polymers, charge control agents, surface additives, wax and other ingredients. The properties of these heterogeneous materials interacting with substrates having variable surface roughness, porosity, and permeability influence the quality and endurance of printing. The surface roughness, adhesion, and wettability of printed surfaces play a key role in the analysis of printing parameters [1, 2, 3].

Nanoscale and microscale features contribute to the spatially heterogeneously distributed physical properties of printing substrates and colorants. Thus, there is a need to characterize them from the nanoscale up. AFM is a high resolution technique, which has been used to image a wide variety of materials with nanometer scale resolution. In particular, it has been employed to measure surface roughness of commercial coated and glossy papers [3, 4, 5] and toner particles [6].

Modern AFM supports a wide variety of functional imaging modes beyond topography imaging. In this work, we present preliminary studies using AM-AFM and 2nd harmonic KPFM, which offer a powerful method for mapping variations in the composition, mechanical and electrical properties of heterogeneous samples [7, 8, 9, 10].

In this work, a study of printed dots is conducted through phase-contrast imaging and quantitative energy dissipation maps, results derived from collected data using AM-AFM. Additionally, measurements of the surface potential and the magnitude of the capacitance gradient between the AFM tip and the samples (printed dots) are presented via 2nd harmonic-KPFM. These provide information of electrical properties such as charge distribution and local dielectric properties.

We investigate three digital printing technologies: electrophotographic with dry toner (HP LaserJet) and liquid toner (HP Indigo), and inkjet, over two printing media: white paper and transparent media. To our knowledge, such a study has not been previously reported.

Materials and methods

Samples and printing technologies

Black dots were printed using three types of digital printers: LaserJet, Indigo, and inkjet. Two types of substrates were used for each printer, a white paper and a transparent media (Dura-Go Clear Polyester Tipped Tekra). As a reference, an optical view of the different printed dots on white paper is shown in Fig. 1. The red boxes indicate the chosen region ($30\mu m x 30\mu m$) for AFM characterization.

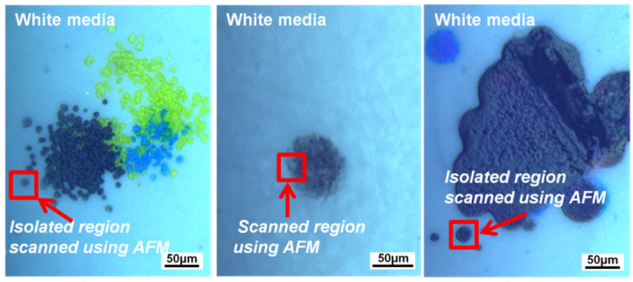

Figure 1. Optical view of printed dots on white paper using a) LaserJet, b) Indigo and c) Inkjet printers. By way of clarification, the template size used to print the dots was not the same for each printer.

LaserJet uses electrophotographic (laser) printing with dry toner to transfer digital data to paper. During this process, the toner powder is electrostatically attracted to charged areas of a photoconductor and then fixed to the substrate with heat and pressure. In this work, we use an HP 125A black LaserJet cartridge, which is a type of HP ColorSphere toners technology.

Indigo involves liquid HP ElectroInk technology. Like LaserJet, HP ElectroInk enables digital printing by electrically controlling the location of the print features. HP ElectroInk is provided as a concentrated paste that is loaded into the press in tubular cartridges. Inside the press it is fed into ink tanks and diluted with oil, to form a fluid mixture of carrier liquid and colorant particles ready for printing [11]. Here, we use HP ElectroInk Mark 4.0 cartridge. During printing, there was no need for backing paper during printing on transparencies as was necessary in the case of the Inkjet or LaserJet.

For our experiment, the inkjet system is based on thermal technology. Inside the printhead, an electrical pulse heats a tiny resistor in a drop generator that is filled with ink. The ink

vaporizes forming a bubble that expands to push a drop out of a nozzle. An HP 980 Ink cartridge based on pigment ink was used in this case. These inks are composed of colorants and a liquid, which is mainly water, but also contains other ingredients for controlling drop ejection and interactions between the ink and the substrate. Once the ink drop is on the substrate, the volatile components evaporate leaving the pigments [12].

Table 1 summarizes the basic information of the three printing technologies used in this work.

Table 1: Printer technologies

Printer	Technology	Cartridge
LaserJet	Dry toner, electrophotographic (laser)	HP 125A Black Toner
Indigo	ElectroInk, electrophotographic (laser)	HP ElectroInk Mark 4.0
Inkjet	Pigment ink, thermal	HP 980 Black Ink

Amplitude modulation atomic force microscopy (AM-AFM)

In this study, AM-AFM is used for quantitative mapping of surface and mechanical properties of the printed dots and the substrates (white paper and transparent media). In this dynamic mode, the AFM micro-cantilever is mechanically excited at a frequency (ω) close to its resonance frequency (ω_0), and the oscillation amplitude is used as a feedback parameter to measure the topography while scanning over the sample surface [7]. The phase lag (φ) between the excitation force and the tip response can be related to image compositional variations in the sample and quantification of mechanical properties.

Two dominant interaction regimes can be distinguished between the tip and the sample, namely, attractive and repulsive. On one hand, in the attractive regime, a net attractive force dominates the amplitude reduction and $\varphi > 90°$. On the other hand, a net repulsive force dominates the repulsive regime and $\varphi < 90°$, usually in intermittent contact with the sample [9].

It is important to appreciate that phase shift variations are related to energy dissipation processes by the tip-surface interaction. The energy dissipated in one cycle by the tip on the sample surface is given by [9, 13]

$$E_{dis} = E_{exc} - E_{med} = \frac{\pi k A_{sp} A_0 sin\varphi}{Q} - \frac{\pi k A_{sp}^2 \omega}{Q \omega_0}, \qquad (1)$$

where E_{exc} is the average energy dissipated by inelastic interactions at the tip-sample interface and E_{med} is the average energy dissipated via hydrodynamic viscous interactions with the environment which in this case was ambient air. The terms A_{sp} and A_0 are the setpoint and free oscillation amplitudes, k and Q are the spring constant and quality factor of the cantilever. Equation (1) is used to convert the phase images into maps of energy dissipation, with $\omega = \omega_0$.

When the tip is intermittently tapping, the phase provides information about the stiffness of the sample surface related to changes in the Young's modulus [8]. Therefore, when analyzing phase-contrast images of heterogeneous substrates, brighter phase lag corresponds to more dissipative and softer material, while darker phase lag corresponds to less dissipative, stiffer material [7, 8].

Topography maps provide information about the roughness of the surface. Two relevant parameters are the maximum roughness and the roughness average (r.a.). The first one corresponds to the maximum value of the height over the sample area scanned. The second is defined as the mean of the difference, in absolute value, between the average height and the height of each single point of the sample. It gives an estimate of how rough is the sample.

2nd harmonic Kelvin Probe Force Microscopy (KPFM)

KPFM is based on the principle of the macroscopic Kelvin probe method to measure contact potential difference, which has been adapted to nanoscale, using the electrostatic force (F_e) as the controlling parameter. As shown in Eq. (2), the electrostatic interaction is proportional to the capacitance gradient $(\partial C/\partial z)$, and the square of the potential difference between the tip and the sample which is composed of i) a compensation dc-voltage (V_{DC}), ii) an ac-voltage (V_{AC}) at a frequency ω_e, and iii) the surface potential difference $V_s(x, y)$ [14].

$$F_e = \frac{1}{2}\frac{\partial C}{\partial z}[V_{DC} - V_s(x,y) + V_{AC}\sin(\omega_e t)]^2. \qquad (2)$$

Expanding Eq. (2), F_e can be separated into three factors: i) a dc, ii) an ω_e, and iii) a $2\omega_e$ frequency components. For surface potential measurements, the relevant term depends on ω_e which is given by

$$F_{\omega_e} = -\frac{\partial C}{\partial z}\left[\frac{1}{2}(V_{DC} - V_s(x,y))^2 V_{AC}\sin(\omega_e t)\right]. \qquad (3)$$

A feedback loop is used to apply a compensation voltage V_{DC} that nullifies the F_{ω_e} component. Thus, knowing V_{DC} the local surface potential of the sample $V_s(x, y)$ can be measured.
Additionally, the 2nd harmonic of the electrostatic force is given by the $2\omega_e$ component ($F_{2\omega_e}$). This signal is used to determine $\partial C/\partial z$, the capacitance gradient, which provides information about the local dielectric properties of the sample. $F_{2\omega_e}$ is expressed as

$$F_{2\omega_e} = \frac{1}{4}\frac{\partial C}{\partial z} V_{AC}^2 \cos(2\omega_e t). \qquad (4)$$

In this work, we use double-pass 2nd harmonic-KPFM. This mode requires two scans, the first records the topography of the sample surface as in AM-AFM. During the second scan, the potential feedback loop is turned on and the bias voltage is applied to the tip, which is lifted by a specified height. The output observables are topography, phase, surface potential and the amplitude response of the second harmonic of the electrostatic force ($A_{2\omega_e}$). From the latter, the magnitude of $\partial C/\partial z$ is obtained using the relation

$$\left|\frac{\partial C}{\partial z}\right| = \frac{4kA_{2\omega_e}}{QV_{AC}^2} \qquad (4)$$

Eq. (4) applies when ω_e is equal to the half of the resonance frequency of the cantilever, enhancing $A_{2\omega_e}$ by the cantilever resonance peak. This derivation is detailed elsewhere [10].

Results

Experimental data using AM-AFM was taken using a silicon micro-cantilever model ACLA from AppNano, with a resonance frequency of *189.9 kHz*, Q = *391* and k = *49.5 N/m*, calibrated

based on the power spectral density during thermally induced motion. The optical lever sensitivity was found via force curve, and repulsive regime was used during imaging with an amplitude setpoint ratio of *~43%*, using A_{sp} = *23nm* and A_0 = *54nm*.

For KPFM data, we used a conductive micro-cantilever model ANSCM-PA from AppNano, with a resonance frequency of *278.5 kHz*, Q = *375* and k = *25.2 N/m*. During the first scan, the amplitude setpoint ratio was *~70%*, and a lift height of *10 nm* was used at the second scan.

All AFM experiments were performed under ambient conditions (20ºC and relative humidity between *30%* and *50%*). The topographic maps presented below are enhanced by a 3-dimensional rendering algorithm that utilizes a directional lighting effect.

Paper comparison

A comparison between the two substrates used in this work is shown in figure 2. From the topography images in Figs. 2a and 2c, it is evident that the transparent media presents a smoother surface compared to the white paper, having a r.a. of *~63.7 nm* compared to *~2.3 nm* for the transparent media. A zoom-in region (Fig. 2b), shows a cellulose-based structure with a non-negligible roughness for the white paper with a maximum roughness of *~200 nm* and a r.a. of *~36.4 nm*, while in an area of the same dimension, the transparent media has a maximum roughness of *~13 nm* and a r.a. of *~1.5 nm*.

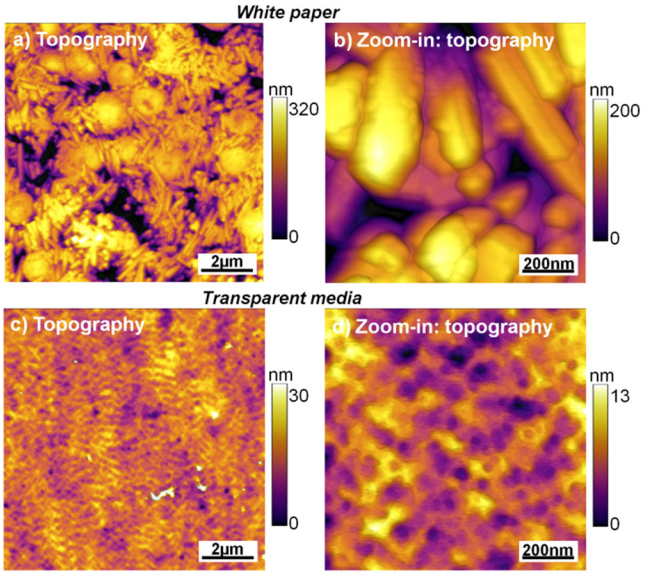

Figure 2. Comparison between white paper and transparent media. Topography of a 10µmx10µm region of a) white paper and c) transparent media. Zoom-in topography: 1µmx1µm region for b) white paper and d) transparent media.

Printed dots analysis: topography phase contrast and energy dissipation maps

LaserJet

Figure 3 presents the results obtained for selected regions on the printed dots using a LaserJet printer. The topography of the *30µmx30µm* region indicated on the optical view of Fig. 1a is shown in Fig. 3a when using white paper as a substrate. As expected, the cellulose based structure, similar to that presented on Fig 2a, can be distinguished around the toner region. In the case of the transparent sheet, an isolated region of the same size was scanned, the topography image is shown in Fig. 3b (optical view not shown here). The roughness of the transparent sheet is negligible compared to the toner features.

The height profiles (labeled P1 and P2 in Fig. 3c) clearly show a difference in the spread and shape of a typical *30µmx30µm* region of the printed dot. Over the white paper it is flatter, wider and non-uniform (P1), while in the transparent sheet it has a well-defined shape (P2) with a maximum height of *~1.4µm* at the center.

The AFM characterization readily allows further magnification by zooming into a *1µmx1µm* region on top of the printed dot. As shown in Fig. 3a, small spherical-shaped particles (tens of nm in diam.) can be distinguished in the topography (Fig. 3d) and phase (Fig. 3e) maps. The phase image exhibits a strong contrast between the particles and the surrounding material. Appearing with a darker contrast, the particles are stiffer and less viscous compared to a softer, more viscous region surrounding the spherical-shaped particles (brighter contrast). This is also validated in the energy dissipation map of Fig. 3e obtained using Eq. (1). Less energy is dissipated over the particles, while a high level of energy dissipation occurs in the material surrounding them.

These results are consistent with the general composition of the HP ColorSphere toner used in this work. The toner is composed of particles (here distinguished at nm scale), that are chemically grown around a wax core, designed for enhanced charge capabilities and more complete melting. Also, there are additives used to enhance the adhesion of the individual toner particles, thus avoiding excess wear while also maintaining toner charge [15]. This heterogeneous composition gives a hint that the material surrounding the particles is comprised of wax and additives.

Indigo

As mentioned above, the HP ElectroInk contains small particles in a fluid mixture of liquid carrier. This technology enables thin image layers which closely follow the surface topography of the paper [11].

The results obtained for selected regions on printed dots using an Indigo printer with HP ElectroInk Mark 4.0 are shown in Fig. 4. In these samples, it was not possible to find isolated regions of small sizes (*<30µm*) like in the LaserJet or Inkjet samples. The printed dot is well shaped and more compact than observed in the other cases.

A topography image of the edge of an Indigo dot corresponding to the region marked on the optical view of Fig. 1b is shown in Fig. 4a. It is difficult to distinguish the boundary between the dot and the paper, due to the roughness of both surfaces. In contrast, the smoothness of the transparent sheet is clearly distinguishable in Fig. 4b and the corresponding height profile P2 in Fig. 4c allows a clear distinction between the two regions (printed feature and substrate).

The zoomed-in images shown in Figs. 4d-e were taken over the colorant region from Fig. 4b. The topography (Fig. 4d) shows a non-uniform and rough surface, while the phase (Fig. 4e) and energy dissipation maps (Fig. 4f) display a strong three color based contrast. Darker features reveal the presence of smaller particles compared to the LaserJet toner (few nm). These particles are stiffer, less viscous and present low energy dissipation (*~100 eV*). Within the material around the dark particles, two color phase contrast can be distinguished, revealing white patches,

corresponding to softer, more viscous layer with more dissipation (*~1200 eV*) and an intermediate component.

Inkjet

Selected regions on dots printed using an Inkjet printer were scanned and the results are shown in Fig. 5. For the white paper and transparent media, isolated regions of the printed feature were studied as shown for the case of white paper in Fig. 1c. For both substrates, the topography images (Figs. 5a-b) allow the distinction of the shape and boundary of the deposited ink and the substrate. However, there is a significant difference when comparing the morphology of the ink. On the paper substrate, the surface of the printed dot is non-uniform as seen from the profile P1 in Fig. 5c, with some paper features in the middle of the ink. Meanwhile, for the transparent media, the deposited ink forms a drop-like feature, as shown by the height profile P2 in Fig. 5c.

For the zoom-in area in Fig. 5d (taken over the ink in Fig. 5b), an uneven rough surface is evident from the topography, with the presence of small particles, which appear in a higher concentration when comparing with the previous cases, over the same size area (1μmx1μm). These particles are attributed to pigments in the ink. Once a drop of the ink is deposited on the substrate, pigments are left behind as the ink vehicle (liquid) evaporates [12].

The phase (Fig. 5e) and energy dissipation maps (Fig. 5f) show a contrast between the stiffer (darker phase), less viscous and less dissipative particles and a softer (brighter), more dissipative component surrounding the particles.

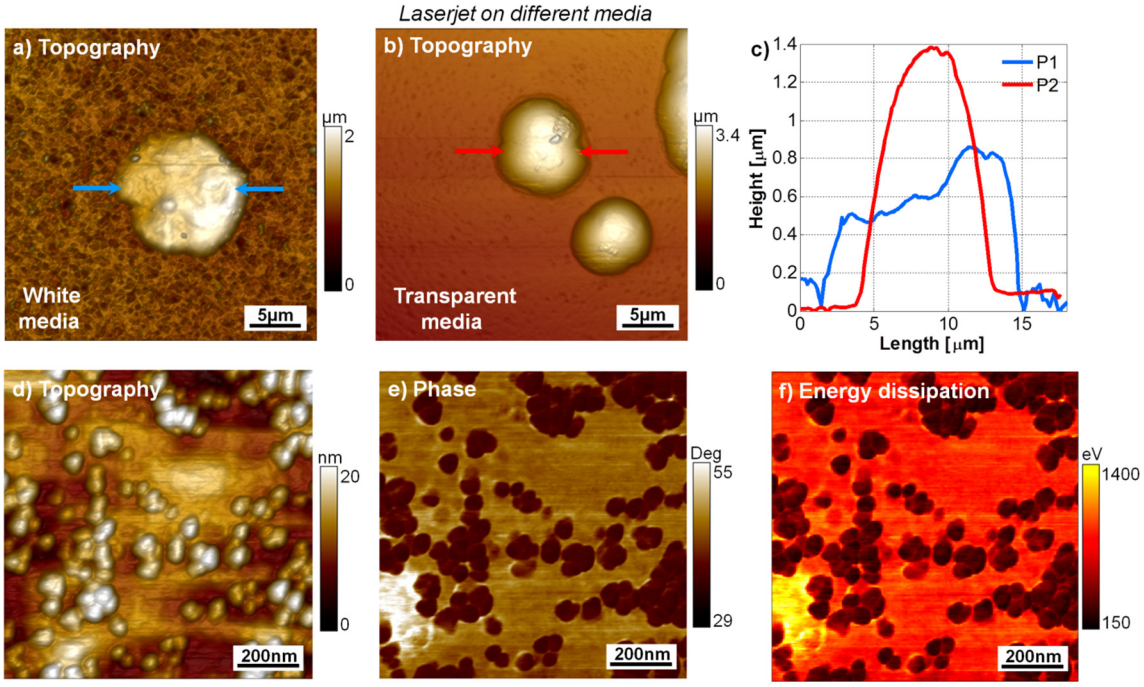

Figure 3.LaserJet printing. First row: topography images (30μmx30μm) showing a comparison between prints on a) white paper and b) transparent media. c) Height profiles taken along the directions indicated by the arrows on a) and b). Second row: Zoom-in over the toner region in a), 1μmx1μm d) Topography, e) phase and f) energy dissipation maps.

Surface potential and capacitance gradient maps

As a way of example, an area of 4μmx4μm of the printed dot with LaserJet technology was used for 2nd harmonic-KPFM measurements. The results are shown in Fig. 6. During the first scan, both topography and phase maps are acquired, in this case showing similar characteristics as in Figs. 3d-e. Topography (Fig.6a) shows the presence of small particles that are clearly distinguished in the phase contrast (Fig. 6b). These are stiffer and less viscous than the surrounding material.

From the second scan, surface potential and $A_{2\omega_e}$ maps are collected, with an ac-voltage at half of the resonance frequency, i.e. $\omega_e = \omega_0/2$. The $A_{2\omega_e}$ map was converted into the magnitude of $\partial C/\partial z$ by means of Eq. 4. Both maps are a useful quantitative tool to understand local electrical properties of the sample, such as charge distribution, dielectric properties, capacitance, etc.

The surface potential map is shown in Fig. 6c and suggests that the small particles have a lower potential (more negatively charged) relative to the surrounding heterogeneous material, which in turn exhibits a non-homogeneous contrast with an appreciable variation in the relative potential values.

In the $|\partial C/\partial z|$ map presented in Fig. 6d, the small particles have low values of capacitance gradient, implying a lower dielectric constant compared to the heterogeneous surrounding region (wax, additives, etc). This map is useful for compositional mapping based on contrast mainly arising from local effective dielectric properties.

Conclusion

AM-AFM and 2nd harmonic KPFM are two powerful techniques for mapping variations in the composition and quantification of mechanical and electrical properties of colorants used in the printing industry, aside from the substrates. Useful surface information can be extracted from the acquired maps, for instance, the volume of individual toner dots and the distribution density of the small particles. Phase contrast contributes to the analysis of mechanical properties and quantification of energy dissipation by tip-sample interactions.

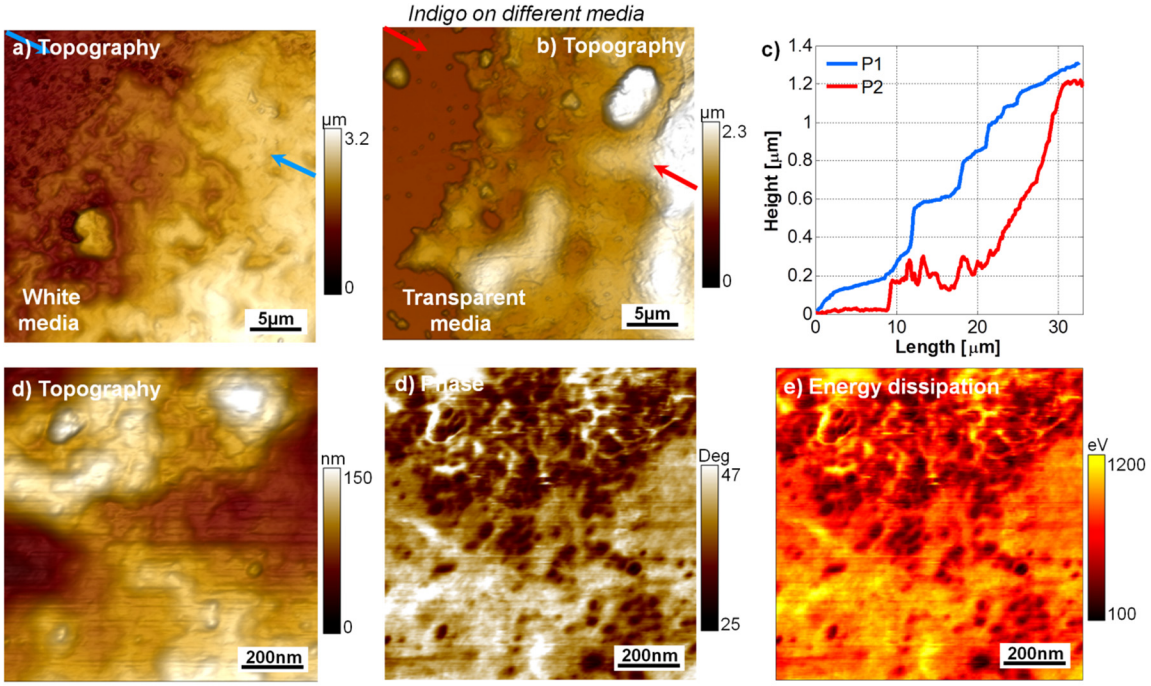

Figure 4.Indigo printing. First row: comparison between prints on different media. Topography images (30µmx30µm) on a) white paper and b) transparent media. c) Height profiles taken along the directions indicated by the arrows on a) and b). Second row: Zoom-in over the ink region in b), 1µmx1µm d) Topography, e) phase and f) energy dissipation maps.

Surface potential and $|\partial C/\partial z|$ maps offers the possibility to study local effective electrical characteristics, such as charge distribution and dielectric properties. Through this exploratory study, we believe functional AFM techniques can be used to extend the characterization and the analysis of colorants and printing substrates to the nanoscale, an advance which could contribute to the improvement of quality in the printing industry.

References

[1] S. Banerjee and D. IanWimpenny, "Laser Printing of Polymeric Materials," in *International Solid Freeform Fabrication Symposium*, Austin, 2006.

[2] R. Xu, A. Pekarovicova, P. Fleming and V. Bliznyuk, "Physical Properties of LWC Papers and Gravure Ink Mileage," *TAPPI Coating Conference and Exhibit,* pp. 365-373, 2005.

[3] R. Xu, P. D. Fleming and A. Pekarovicova, "The Effect of Ink Jet Paper Roughness on Print Gloss," *J. Imaging Sci. Technol.,* vol. 49, no. 6, pp. 660-666, 2005.

[4] M.-C. Beland and J. M. Bennett, "Effect of local microroughness on the gloss uniformity of printed paper surfaces," *Appl. Opt.,* vol. 39, no. 16, pp. 2719-2726, 2000.

[5] R. Xu, Y. J. Wu, A. Pekarovicova, P. D. Fleming and M. X. Wang, "The Effects of Paper Coating on Gravure Ink," *Proceedings of the Technical Association of the Graphic Arts, TAGA,* pp. 517-526, 2007.

[6] JPK Instruments, "Studying texture of paper with AFM and upright optical microscopy using the BioMAT workstation," JPK Instruments AG.

[7] R. Garcia and R. Perez, "Dynamic atomic force microscopy methods," *Surf. Sci. Rep.,* vol. 47, pp. 197-301, 2002.

[8] S. N. Magonov, V. Elings and M. H. Whangbo, "Phase Imaging and stiffness in tapping-mode atomic force microscopy," *Surf. Sci. Lett.,* vol. 375, pp. L385-L391, 1997.

[9] N. F. Martinez and R. Garcia, "Measuring phase shifts and energy dissipation with amplitude modulation atomic force microscopy," *Nanotechnology,* vol. 17, pp. S167-S172, 2006.

[10] X. Xu, J. Mares, L. J. Groven, S. F. Son, R. G. Reifenberger and A. Raman, "Nanoscale characterization of mock explosive materials using advanced atomic force microscopy methods," *J. Energ. Mater.,* vol. 33, pp. 51-65, 2015.

[11] Hewlett-Packard Development Company L.P, "HP ElectroInk," 2009.

[12] Hewlett-Packard Development Company, L.P., "HP PageWide technology breakthrough speed, professional quality," 2012.

[13] B. Anczykowski, B. Gotsmann, H. Fuchs, J. P. Cleveland and V. B. Elings, "How to measure energy dissipation in dynamic mode atomic," *Appl. Surf. Sci.,* vol. 140, pp. 376-382, 1999.

[14] S. Sadewasser and T. Glatzel, Kelvin Probe Force Microscopy: measuring and compensating electrostatic forces, Springer Ser. Surf. Sci., 2012.

[15] Hewlett-Packard Development Company L.P, "HP ColorSphere toner Innovative technology for high-impact color results," 2005.

Author Biography

Maria J Cadena received her MS in electronic engineering from the University of Los Andes (Colombia) in 2012. Since 2013, she is a PhD student in mechanical engineering at Purdue University. She is working in the research group of Dr. Raman and Dr. Reifenberger at Birck Nanotechnology Center. Her research is focused on the development of functional quantitative dynamic atomic force microscopy techniques, particularly in the field of electrical characterization applied to heterogeneous materials.

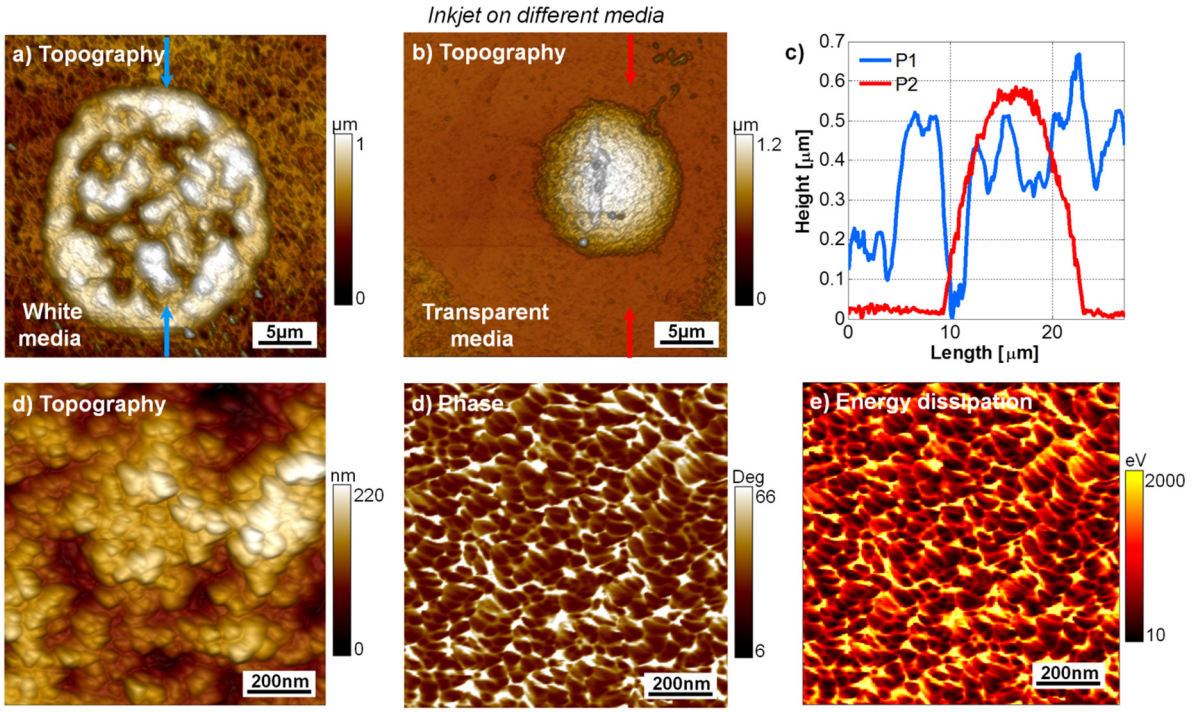

Figure 5.Inkjet printing. First row: comparison between prints on different media. Topography images (30μmx30μm) on a) white paper and b) transparent media. c) Height profiles taken along the directions indicated by the arrows on a) and b). Second row: Zoom-in over the ink region in b), 1μmx1μm d) Topography, e) phase and f) energy dissipation maps.

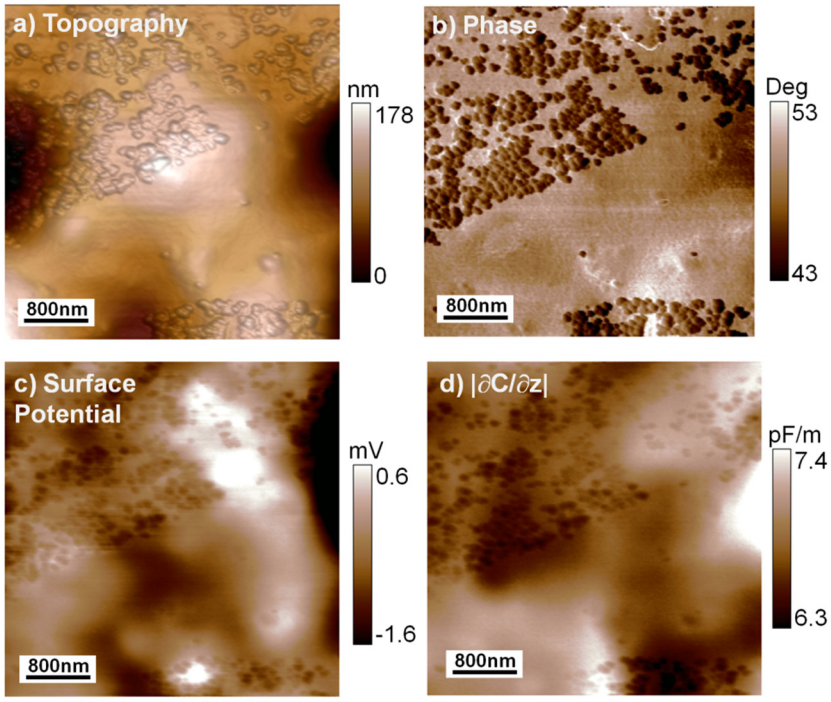

Figure 6. KPFM observables of a 4μmx4μm area of the printed dot using LaserJet on white paper. a) Topography, b) phase, c) surface potential and d) Magnitude of the capacitance gradient. These images were taken using double-pass mode. Topography and phase were recorded during the first scan, while surface potential and |∂C/∂z| corresponds to the outputs during the second pass with the following parameters: $V_{AC} = 8V, \omega_e = 139.29kHz, 2\omega_e = 278.58kHz$ *and lift height = 10nm.*